Available online at www.sciencedirect.com
ScienceDirect
Surface Science 600 (2006) 4813–4824
SURFACE SCIENCE
www.elsevier.com/locate/susc

Structural characterisation of ultra-thin VO_x films on $TiO_2(1\,1\,0)$

E.A. Kröger [a], F. Allegretti [b], M.J. Knight [b], M. Polcik [a], D.I. Sayago [a], D.P. Woodruff [b,*], V.R. Dhanak [c]

[a] *Fritz-Haber-Institut der Max-Planck-Gesellschaft, Faradayweg 4-6, D 14195 Berlin, Germany*
[b] *Physics Department, University of Warwick, Coventry CV4 7AL, UK*
[c] *CCLRC Daresbury Laboratory, Daresbury, Warrington WA4 4AD, UK*

Received 7 June 2006; accepted for publication 31 July 2006
Available online 18 August 2006

Abstract

The normal incidence X-ray standing wave (NIXSW) technique has been applied to investigate the structure of ultra-thin VO_x films grown on $TiO_2(1\,1\,0)$ and pre-characterised by core level photoemission. For a film composed of a sub-monolayer coverage of V deposited in ultra-high vacuum the local structure of two coexistent species, labelled 'oxidic' and 'metallic', has been investigated independently through the use of chemical-shift-NIXSW. The 'oxidic' state is shown to be consistent with a mixture of epitaxial or substitutional sites and chemisorption into sites coordinated to three surface O atoms. The metallic V atoms also involve a mixture of chemisorption and second-layer sites above the substrate surface consistent with the formation of small V clusters. VO_x films up to ~6 atomic layers were also grown by post-oxidation (sequential V deposition and annealing in oxygen) and by reactive evaporation in a partial pressure of oxygen. While films of around one monolayer or less are consistent with epitaxial VO_2 growth, the film quality deteriorates rapidly with increasing thickness and is worse for reactive evaporation. A possible interpretation of the NIXSW data is increasing contributions of V_2O_3 crystallites. The inferior quality of the reactively evaporated films may be due to an insufficient supply of oxygen.

Keywords: X-ray standing waves; Titanium oxide; Vanadium oxide; Surface structure

1. Introduction

The physical and chemical properties of vanadium oxides display considerable complexity and utility [1,2]. They are widely used in heterogeneous catalysis [3], commonly supported on other oxide materials including, in particular, TiO_2, and it is now recognised that such supports can have significant influence on the catalyst activity through structural, morphological, electronic or chemical interactions. It is therefore not surprising that there have been quite a number of detailed surface science studies of vanadium oxides [4], and in particular of ultra-thin films grown on TiO_2, of which the simplest model surface for such investigations is the rutile (1 1 0) single crystal surface. This system seems to have been first studied by Zhang and Henrich [5], but currently the main structural information comes from Granozzi and coworkers who have carried out extensive studies of this growth system under different growth conditions and at different film thicknesses from sub-monolayer coverage to tens of atomic layers [6–11]; a review published in 2001 summarises this early work [12], but does not cover the results of a more recent collaboration with Netzer and coworkers [13,14]. Other groups have also made important contributions to investigations of this growth system [15–19].

From the point of view of structural characterisation of these films, an important feature of the work of the Granozzi group has been the use of X-ray photoelectron diffraction (XPD), exploiting forward scattering of high energy

* Corresponding author. Tel.: +44 2476523378; fax: +44 2476692016.
E-mail address: d.p.woodruff@warwick.ac.uk (D.P. Woodruff).

0039-6028/$ - see front matter © 2006 Elsevier B.V. All rights reserved.
doi:10.1016/j.susc.2006.07.049

photoelectrons produced by a conventional laboratory XPS MgK_α X-ray source. Under most growth conditions these XPD data were found to indicate the growth of epitaxial VO_2, despite the fact that the low energy electron diffraction (LEED) observations for some of these films indicated a lack of long-range order rather than the expected (1×1) pattern. The lattice mismatch between rutile phase TiO_2 and VO_2 is small (3.5% along [0 0 1], 1% along $[1\,\bar{1}\,0]$), so pseudomorphic growth is likely on purely geometrical considerations. Some apparently conflicting evidence, however, comes from investigation of the electronic structure of these films both through chemical shifts in the core level photoemission (XPS), and from valence band photoemission. Much of the associated debate concerns the interpretation of the values of the V $2p_{3/2}$ photoelectron core level binding energy measured in these experiments. Even the values of this parameter for reference spectra from bulk oxides of difference valency (notably V^{5+} in V_2O_5, V^{4+} in VO_2, V^{3+} in V_2O_3, V^{0+} in metallic vanadium) have not been without dispute, in part due to the use of different reference energies (see, for example, Refs. [20,21] and references therein). However, it seems to be generally accepted that the V $2p_{3/2}$ binding energies seen in XPS from the oxide films prepared on TiO_2(1 1 0) commonly have values which might be more consistent with the V^{3+} value of bulk V_2O_3 than the V^{4+} value of bulk VO_2, although these energies only differ by about 0.5 eV and so need careful absolute referencing. To counter this apparent discrepancy, it has been argued that the fact that the films are very thin, or in small particles (STM results [13,14,17] show the thinnest films, at least, are far from homogeneous) may lead to modified photoelectron binding energies. Vibrational spectroscopic data have been interpreted in terms of V_2O_3 [15] and VO_2 [18] film growth in different studies. Wang and Madix have also shown that they can prepare films with an XPS spectrum characteristic of V_2O_5 (V^{5+}), by a novel deposition route involving reaction with $VOCl_3$ and water vapour [22], but using the more standard route of V metal deposition and oxidation during, or after, deposition, only one paper claims to identify this higher valency oxide growth [19].

Our interest in this growth system was initiated by a desire to investigate the structure of adsorbates on VO_2 surfaces using scanned-energy mode photoelectron diffraction (PhD) [23]. However, in a series of PhD experiments (unpublished) based on thin vanadium oxide films on TiO_2, grown under conditions similar to those reported to form epitaxial VO_2 on the basis of XPD measurements, we obtained results which cast doubt on the crystalline quality and nature of these films. We have therefore undertaken an investigation of these films using normal incidence X-ray standing waves (NIXSW), a method [24,25] better suited to investigate the structural quality of thin pseudomorphic epitaxial films. In particular, we report here the results of NIXSW measurements to investigate the structure of two distinct types of deposited films. The first of these gives some insight into the earliest stages of vanadium oxide growth on TiO_2(1 1 0), achieved by studying an as-deposited sub-monolayer coverage of metallic V onto the surface, leading to at least two distinct coexistent surface forms of V identified, via the V 2p core level shifts, as 'metallic' and 'oxidic' [5,7,17]. The second set of samples are of films intended to be epitaxial oxide with average thicknesses of a few atomic layers produced either by successive deposition of small amounts of V metal followed by annealing in an oxygen partial pressure ('post-oxidation' or 'PO') or by V deposition in a partial pressure of oxygen ('reactive evaporation' or 'RE'). All of the original XPD work of the Granozzi group used the PO mode of growth, but a more recent STM study in collaboration with the group of Netzer indicates [14] that, at least for the thinnest films, the film quality may be superior for RE growth.

2. Experimental details, pre-characterisation and NIXSW methodology

The NIXSW experiments were conducted on the double crystal monochromator beamline 4.2 of the Synchrotron Radiation Source at the CLRC's (Central Laboratories for the Research Councils) Daresbury Laboratory. This beamline has been described in detail elsewhere [26,27]; it is fitted with a pair of InSb(1 1 1) Bragg reflectors and a surface science end-chamber equipped with the usual *in situ* sample preparation and characterisation facilities. A concentric hemispherical analyser (with the entrance lens at 40° to the incident photon beam in the horizontal plane) was used to measure the energy distribution curves (EDCs) of photoemitted and Auger electrons at fixed pass energy. Core-level X-ray photoelectron spectroscopy (XPS) to characterise the surface used the same analyser, in combination with a conventional MgK_α X-ray source (photon energy 1253.6 eV), or with the monochromated synchrotron radiation beam, generally using a photon energy of 1919 eV.

A clean well-characterised rutile TiO_2(1 1 0) surface was prepared *in situ* by cycles of Ar ion bombardment (10 μA, 0.5 keV) and heating (by electron bombardment of the sample back-plate) to 600 °C. This gave a sharp (1×1) LEED pattern and a Ti 2p photoemission spectrum characteristic of an essentially defect-free surface. The main Ti 2p peaks are generally assigned to Ti in the 4+ charge state expected for a fully ionic stoichiometric bulk site and in the autocompensated surface (e.g. [28]), while any high kinetic energy shoulder is assigned to Ti in a 3+ state, most commonly attributed to the presence of surface oxygen vacancies. VO_x films on the surface were grown using a water-cooled V wire electron-beam evaporator. In the case of films grown by reactive evaporation (hereafter referred to as RE) the growth was effected at a sample temperature of ~200 °C with evaporation in a partial pressure of oxygen of 5×10^{-8} mbar at a rate of approximately 0.6 MLE/min, where 1 MLE (monolayer equivalent) corresponds to the V coverage in one layer of a pseudomorphic

VO_2 phase on $TiO_2(1\,1\,0)$ (i.e. equivalent to the Ti atomic density in one layer of this TiO_2 surface). For the post-oxidation (PO) growth, a sequence of deposition and oxidation cycles was used, the V being deposited in aliquots of approximately 0.5 MLE onto the sample at room temperature, followed by annealing to ~200 °C for ~2 min in a partial pressure of oxygen of 1×10^{-6} mbar. In most cases the RE growth was also conducted in short incremental deposits of ~0.5 MLE, although single longer doses were also tested and produced very similar films as judged by the NIXSW data.

The effective thickness of these films was assessed on the basis of the relative intensities of the V 2p and Ti 2p photoemission peaks using the MgK_α X-ray source, which was also used as a means of calibrating the evaporation rate. This method of determining the coverage is, of course, susceptible to ambiguity if the growth mode is not known. Our procedure, using the attenuation length of the Ti 2p photoelectrons in the VO_x film at a kinetic energy of ~790 eV to be 15 Å [29], relies on the assumption that the film is homogeneous and thus, in effect, that the growth is layer-by-layer. In fact the published STM images show clearly that this is not the case for the very thinnest ($\leqslant$1 MLE) films, and our measurements for the PO and RE films showed different degrees of Ti 2p attenuation for similar V 2p signals, suggesting that the morphology of the films resulting from the two different growth modes may be significantly different. The film thicknesses quoted here should therefore be regarded as indicative only (perhaps no better than ±50%), but this limitation does not prevent us drawing conclusions regarding the qualitative trends in changes in the film crystallography with increasing thickness.

The NIXSW technique [24,25] is a variant of the general X-ray standing wave method [30] in which one exploits the X-ray standing wave set up at an X-ray Bragg scattering condition in the crystalline substrate due to the interference of the incident and diffracted beam. This standing wavefield has a periodicity equal to that of the associated substrate scattering planes, and shifts in phase relative to the scattering atoms in a systematic and predictable fashion as one scans through the Bragg condition, either in incidence angle (a so-called rocking curve) or in photon energy (wavelength). By measuring the X-ray absorption at a particular atomic species through such a scan one obtains an absorption profile characteristic of the location of the absorber relative to the (extended) scattering planes. At an arbitrary incidence angle the rocking curve width is extremely narrow, precluding the use of the method for all but the most perfect crystals, but at normal incidence to the scatterer planes this problem is relaxed and the NIXSW method can be applied to a much wider range of materials [31]. While an NIXSW measurement at a single Bragg condition provides information on the spacing of an absorber relative to a single set of extended scatterer plane positions, additional measurements of such layer spacings for two or more sets of (non-parallel) scatterer planes allows the absolute location of the absorber to be established by triangulation.

In the case of adsorbed species or ultrathin layers on a surface the variation of the X-ray absorption in the overlayer atoms can be monitored by detecting the changes in the intensity of the photoemission or subsequent Auger electron emission resulting from the photoionisation (photoabsorption). If the photoemission signal is used, the 'chemical shifts' in the photoelectron binding energy, widely exploited in conventional X-ray photoelectron spectroscopy (XPS) allow one to separate the absorption profiles for atoms of the same element in different chemical states [32–34]; in the present case this allowed us to distinguish the 'oxidic' and 'metallic' V species following UHV deposition of vanadium onto the TiO_2 surface without post-oxidation. Notice, though, that there is no detectable core-level shift between the O 1s emission from the TiO_2 substrate and the VO_x species in the films, so monitoring the O absorption provided no useful information. Photoemission detection of the X-ray absorption in XSW requires special precautions in the data analysis; non-dipole effects in the photoemission create a forward/backward asymmetry in the angular dependence of the photoemission relative to the direction of photon propagation. This means that the photoemission from the incident and reflected X-rays are not detected in an equivalent fashion by a detector having a finite acceptance angle [35]. However, for emission from core level s-states, this problem now seems to be well understood [36], and the method of data analysis can be modified to account for this effect [37]. For emission from states of higher orbital angular momentum quantum numbers (notably p-states), a fully quantitative treatment of these effects is not available and only approximate methods can be used. For the present experiments, the most convenient way to monitor the absorption of the X-ray standing wavefield in the overlayer and substrate is by measurement of the V 2p and Ti 2p photoemission intensities, for which the photoionisation cross-section is quite high, but for which this formal problem of a correct description of the non-dipole contribution to the angular dependence of the photoemission is unsolved. However, it is also possible to measure the Ti 2s and V 2s photoemission intensity, for which the non-dipole effects are well-understood, although the cross-section for these states is much lower. While the 2p photoemission signals were therefore used for the bulk of the measurements reported here, a significant number of films were also monitored with 2s emission. We also note that the non-dipole effects for 2p photoemission from Ti and V (adjacent in the periodic table) at the same photon energy are likely to be very similar, so applying the same forward/backward asymmetry parameters to the V 2p data to those found to give a good description of the Ti 2p data from the TiO_2 substrate (of known bulk structure) can be expected to yield rather precise structural parameter values. The checks using the Ti 2s and V 2s photoemission provided added confirmation of this conclusion.

These experimental NIXSW profiles were analysed using the XSWfit automated fitting procedure.[1] NIXSW analysis provides two structural parameters [24,25,30]: the coherent position d_H (where H specifies the Miller indices of the scatterer planes) and the coherent fraction f_{co}. In the simplest case of an absorber occupying a single well-defined site, d_H is equal to the perpendicular distance of this site from the scattering planes, while f_{co} is a measure of the degree of local order. Notice that d_H is defined relative to the nearest extended scatterer plane, so even in this simplest structural situation the real distance may differ from the coherent position by an integral number of substrate interlayer spacings. More generally, f_{co} can only take values between 0 and 1; some reduction below the ideal value of 1 for a single well-defined site to ~0.8–0.9 arises from dynamic (thermal vibrations) or static local disorder. Much lower values can occur, but this generally implies that there is multiple site occupation. The shape of the profiles is also influenced by two non-structural parameters, the Gaussian instrumental broadening ΔE (mainly due to the finite resolution of the monochromator) and the absolute energy of the Bragg reflection E_B. These parameters can be determined by fitting the substrate standing wave profile and are then fixed for the analysis of the adsorbate absorption profiles, which are then fitted by only adjusting the adsorbate structural parameters.

For a more general understanding of the relationship between the XSW structural parameters of the coherent position and coherent fraction, and the actual positions of absorber atoms, a rather more formal discussion is required. In particular, to analyse situations involving two or more distinct absorber sites one exploits the finding that the coherent fraction and coherent position can be related to the spatial distribution of the absorber atoms relative to the nearest scatterer plane $f(z)$, defined by the spacing coordinate z, by

$$f_{co}\exp(2\pi i d_H) = \int_0^{d_H} f(z)\exp(2\pi i z/D_H)\,dz \qquad (1)$$

where D_H is the bulk interlayer spacing of the H scatterer planes [24,25,30]. From this it is clear that f_{co} and d_H define the amplitude and phase of one Fourier component of the absorber site distribution projected along one direction (perpendicular to the relevant Bragg scatterer planes). Notice that the left hand side of this equation can be represented as a vector in an Argand diagram with length f_{co} and direction determined by the phase angle $2\pi d_H$ relative to the positive real axis [38]. The right hand side of the equation is then a summation (integral) over component vectors of length $f(z)$ and phase angle $2\pi z/d_H$. This interpretation is particularly useful in summing over discrete sites (when $f(z)$ comprises a series of essentially discrete values).

For the case of TiO_2 this summation is even relevant for the bulk three-dimensional crystal, because there are several atoms in the atomic basis. Thus, for the (1 1 0) Bragg reflection the scatterer planes are centred on the Ti atoms, and all the Ti atoms lie in these planes, so an XSW absorption profile based on detection of Ti Auger or photoelectron emission is expected to yield a coherent position of 1.0 (or equivalently, 0.0) with a coherent fraction for a perfect non-vibrating crystal of 1.0 (which will be lowered by ~10–20% in reality). However, half of the O atoms in TiO_2 lie in the same (1 1 0) planes as the Ti atoms, but the other O atoms are placed symmetrically on either side of this plane of atoms at a distance from this plane which is quite close to (but not equal to) one half of the interplanar spacing. This leads to a coherent position of 1.0, (being the average position of the atoms) but a coherent fraction (even for a perfect rigid crystal) of only 0.14. To understand this very low value of the coherent fraction, consider the implications of Eq. (1) for a sum over two atomic positions which differ in their z values by half the interplanar spacing, $D_{hkl}/2$:

$$f_{co}\exp(2\pi i d_H) = \frac{1}{2}[\exp(2\pi i z/D_H) + \exp(2\pi i\{z + D_H/2\}/D_H)]$$

whence

$$f_{co}\exp(2\pi i d_H) = \frac{1}{2}[\exp(2\pi i z/D_H) - \exp(2\pi i z/D_H)] = 0$$

so the coherent fraction is zero and the coherent position is indeterminate (meaningless). Within the Argand diagram representation this is equivalent to summing two equal and opposite vectors. This example highlights the fact that regarding the coherent fraction only as a measure of disorder may be very misleading; a completely disordered (or incommensurate) surface layer can give a coherent fraction of zero, but so can a highly ordered surface with certain specific values of the atomic positions. This source of a strong reduction in the coherent fraction is probably highly relevant to some of the results discussed in the following section.

In order to assess the crystalline structure of the VO_x films as a function of thickness, measurements were made mainly of absorption at the vanadium atoms in the (1 1 0) NIXSW at a photon energy of ~1912 eV. If the film comprises pseudomorphic rutile-phase VO_2, successive planes of V atoms will lie at interlayer spacings only very slightly different from those in bulk TiO_2, which should result in a slow but gradual change in the positions of the V atoms relative to the extended bulk scattering planes of the XSW, retaining the lateral registry of the substrate. Indeed, based on the equations above it is clear that a summation of a series of z values each differing by slightly less than D_H will lead to a coherent position decreasing from 1.0 with a corresponding decrease in the coherent fraction. In this case

[1] XSWfit is a procedure, written as an Igor-Pro macro, which automatically fits XSW data. It is based on the formalism originally developed by D.P. Woodruff in Fortran for calculating the XSW profile for a given set of parameters. A copy of the Igor routines can be obtained from Rob Jones, email: robert.g.jones@nottingham.ac.uk.

triangulation with other scattering planes may be expected to give limited additional information. For the lowest V coverages, however, and particularly for the low coverage V deposition without oxidation, the adsorption sites of the V atoms are completely unknown and triangulation is potentially crucial. For these samples, additional NIXSW experiments were conducted using the (1 0 1) reflection at a photon energy of ~2500 eV. (1 0 1) measurements were also made for a sub-set of the thicker films for completeness.

3. Results and structure determination

3.1. Clean $TiO_2(110)$ NIXSW

In view, particularly, of the need to check on the different modes of monitoring the NIXSW absorption profiles in the VO_x layers, extensive initial tests were conducted on the clean TiO_2(1 1 0) surface, monitoring the Ti 2p, Ti 2s and O 1s photoemission signals and the Ti LMM Auger electron emission at 376 eV kinetic energy. The photoemission signals provided a basis for an empirical determination of the forward/backward asymmetry parameter, Q [35,37] relevant to these experiments which, for the Ti 2s emission, could be compared with the theoretically predicted value [39]. The Ti Auger signal provides a direct measure of the Ti NIXSW absorption profile unclouded by issues arising from the non-dipole asymmetry effects in photoemission. Representative results of these experiments (performed at both the (1 1 0) and (1 0 1) reflections), are shown in Fig. 1. For the (1 1 0) reflection the results yielded consistent fits with $d_H = 1.0$ and coherent fraction values of 0.90 and 0.14 for the Ti and O absorption. For the (1 0 1) reflection the equivalent values were 0.90 and 0.33, the latter value being almost identical to the theoretical value of 0.34 for a perfect crystal. The Q values for the Ti 2s and O 1s emissions were 0.07 and 0.16, also consistent with expectations, while for the Ti 2p a value of 0.15 was obtained. Notice that, in these measurements, the intensity of the inelastically scattered background electron emission also provides a monitor of the substrate absorption. In investigations of elemental solids with a single-atom atomic basis (such as the fcc metals Cu and Ni), the NIXSW measurements based on this background signal leads to structural parameter values equivalent to those found by monitoring absorption at the constituent atoms by Auger electron or photoelectron emission. In the case of TiO_2, this background emission signal contains contributions from both Ti and O absorption, and thus while these absorption profiles can be fitted to coherent position values of unity, the associated coherent fractions are somewhat reduced due to contribution with a low coherent fraction from the (weaker) absorption at the O atoms.

As remarked above, in the studies of the VO_x overlayers the photoemission forward/backward asymmetry parameter for the V 2p emission was set to the same value as that found for the Ti 2p emission, though the resulting structural parameter values proved rather insensitive to this (small) value. In these measurements the bulk absorption profile, used as the reference for the absolute energy scale and the incident photon energy spread, was taken from the inelastically scattered electron background signal, although for the thinner films, at least, direct measurements of the Ti atomic absorption profiles were also made and provided additional checks.

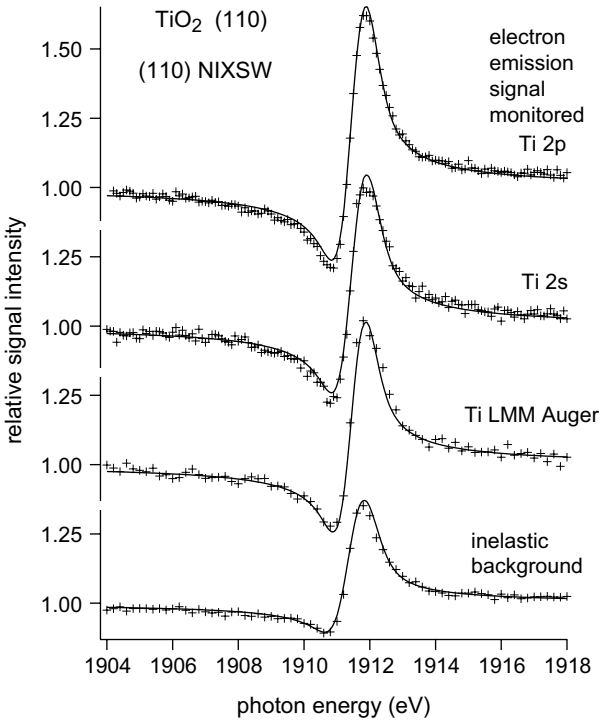

Fig. 1. NIXSW (1 1 0) absorption profiles for clean TiO_2(1 1 0) monitored using different electron emission signals: Ti 2p and Ti 2s photoemission, Ti LMM Auger electron emission, inelastically scattered electron emission background signal at a kinetic energy of ~390 eV. The crosses are the experimental data points, the smooth lines are the theoretical fits.

3.2. Sub-monolayer V on $TiO_2(110)$

Experiments were first conducted on the behaviour of the earliest stages of V deposition, corresponding to the reaction of approximately 0.3 MLE of V with the TiO_2(1 1 0) surface at room temperature with no annealing or oxygen exposure. Fig. 2 shows the V $2p_{3/2}$ photoemission spectrum recorded using the incident synchrotron radiation at a nominal photon energy of 1919 eV. While the instrumental resolution and signal-to-noise ratio is relatively poor, it is clear that there are (at least) two chemically shifted components, consistent with earlier published XPS spectra from surfaces prepared in a similar way. Higher resolution data taken at lower photon energies using the BESSY facility in Berlin (unpublished) showed no significant narrowing of these spectral peaks. For comparison, Fig. 2 also shows a similar spectrum from VO_x films of increasing thickness on the surface grown by both the PO and RE methods. If we assume that the O 1s core

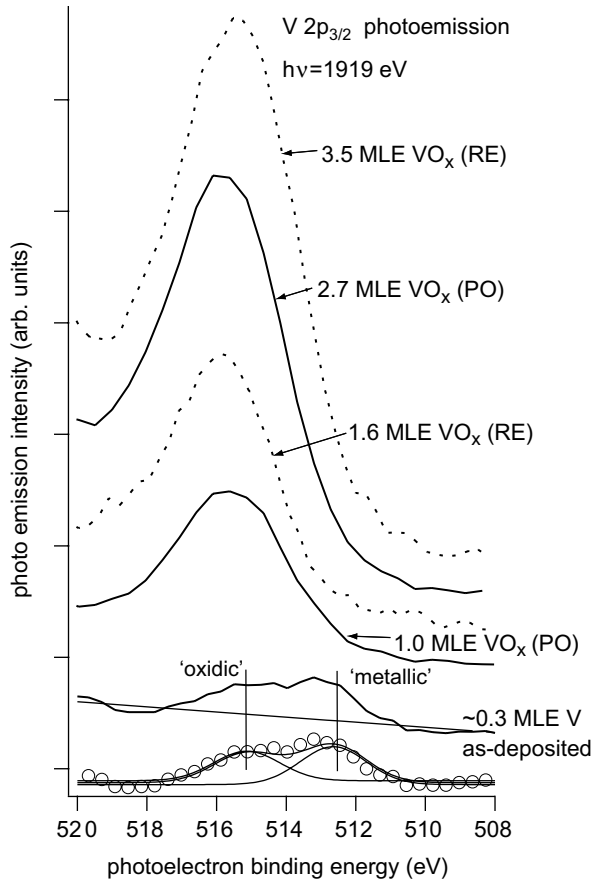

Fig. 2. V $2p_{3/2}$ photoemission spectrum for the as-deposited ~0.3 ML V layer on TiO_2(1 1 0) compared with similar spectra from VO_x films of different thicknesses, two prepared by the post-oxidation method and two by reactive evaporation. All spectra are aligned to a common O 1s photoelectron binding energy value of 529.9 eV. At the bottom is shown the separation of the spectrum from the sub-monolayer as-deposited V film into two components ('oxidic' and 'metallic') after subtraction of a linear background; in this case only the individual experimental data points are shown as circles to distinguish them from the line showing the sum of the two components.

level binding energy in this surface is 529.9 eV (within 0.1 eV of the value found in almost all studies of vanadium oxides as reported in Ref. [21]) then the two V $2p_{3/2}$ binding energies are 514.9 eV and 512.4 eV, similar to the values reported for this surface by the Granozzi [7,9] and Madix [17] groups. As remarked earlier, these two peaks are rather loosely labelled 'oxidic' and 'metallic', respectively; the energy separation is several tenths of an eV less than that expected for a true metallic state and either V_2O_3 or VO_2, but this has been attributed to the influence of the small particles of metal that are likely to be associated with the metallic state [17]. Notice, too, that the thicker fully oxidised films appear to have a V 2p photoelectron binding energy slightly larger than the oxide component from the low-coverage as-deposited V film, although there is some variation in the peak energy for the different oxide film preparations. Fig. 2 also shows that, even at the inferior resolution of these higher energy measurements, the V $2p_{3/2}$ peak from the thicker films is much broader than the two individual components of the sub-monolayer film, irrespective of whether the growth was by the PO or RE methods. This may imply inhomogeneity in the V–O coordination and valency within these films. The V atoms contributing to the oxidic peak in the as-deposited layer have previously been interpreted as occupying substitutional Ti sites within the TiO_2 surface, the XPD results specifically favouring occupation of the surface 6-fold coordinated sites but not deeper sub-surface sites [7]. The displaced Ti atoms produced by this partial substitution, which is consistent with the relative oxygen affinities of Ti and V [40], lead to the appearance of a shoulder in the Ti 2p photoemission spectra nominally associated with Ti^{3+} species.

Chemical-state specific NIXSW for the (1 1 0) reflection based on these V $2p_{3/2}$ photoemission components clearly shows that the local structural environment of the V atoms contributing to these two peaks is different; Fig. 3 shows how the relative intensities of the two peaks change as the photon energy is stepped through the standing wave region. Notice that although the spectral resolution is insufficient to clearly resolve the two components, the two-peak fitting is heavily constrained to have constant widths and constant energy separation for all of the 60 or 80 spectra used in the measurement, with only the intensities of the two peaks being allowed to vary. The NIXSW absorption profiles for the two components resulting from this procedure for both the (1 1 0) and (1 0 1) reflections are shown in Fig. 4, together with the theoretical fits, while the structural parameter values for these fits are shown in Table 1.

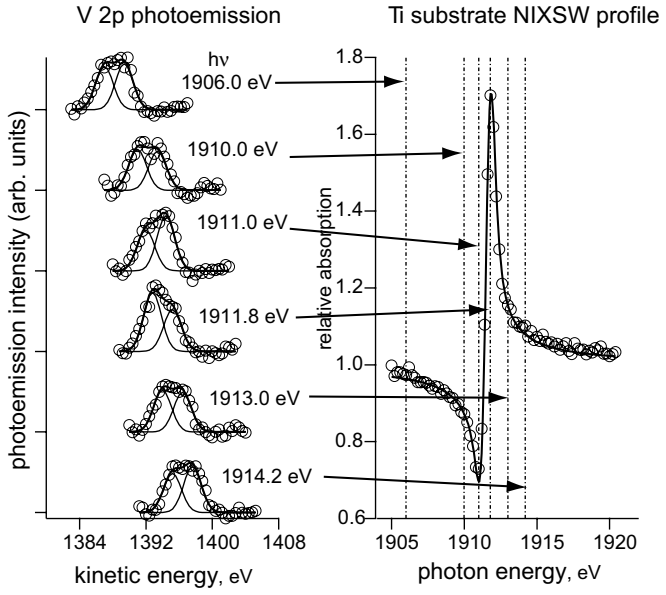

Fig. 3. Composite figure showing the changing shape of the V $2p_{3/2}$ photoemission spectrum at different photon energies within the (1 1 0) NIXSW from a sub-monolayer coverage (~0.3 MLE) of vanadium deposited in UHV on TiO_2(1 1 0). Also shown are the two component chemically shifted peaks identified as 'oxidic' and 'metallic' (see Fig. 3). The changing relative amplitudes of these components are due to the different atomic sites and thus different associated NIXSW profiles.

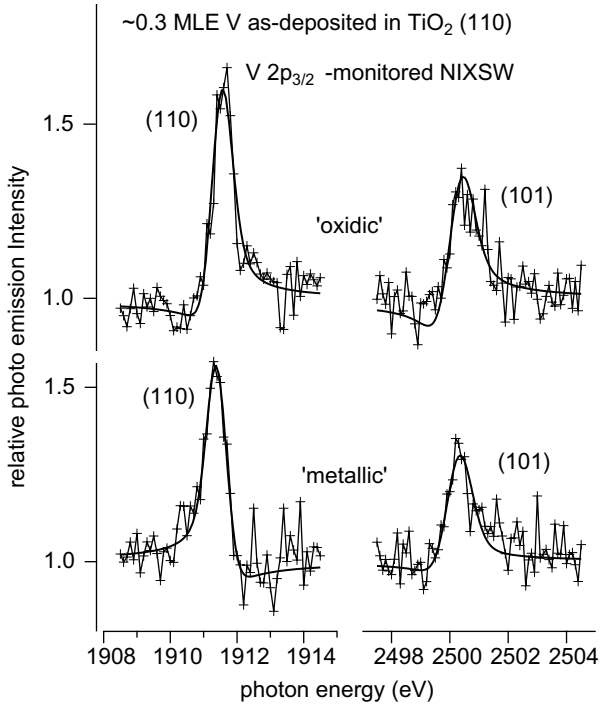

Fig. 4. (110) and (101) NIXSW profiles measured using the two chemically shifted V $2p_{3/2}$ photoemission component intensities from the sub-monolayer coverage of as-deposited V on TiO_2(110). The crosses joined by thin lines are the experimental data points while the smooth bold lines are the theoretical fits, yielding the structural parameter values listed in Table 1.

Table 1
NIXSW fitting parameter values for the as-deposited layer of ~0.3 MLE of vanadium

Reflection	'Metallic' V 2p peak		'Oxidic' V 2p peak	
	d_H	f_{co}	d_H	f_{co}
(110)	0.64 ± 0.10	0.28 ± 0.06	1.00 ± 0.03	0.25 ± 0.10
(101)	1.00 ± 0.03	0.40 ± 0.10	0.08 ± 0.06	0.66 ± 0.12

The quoted precision estimates are based on the scatter of several independent measurements. Note that, as defined in Eq. (1), all d_H values are dimensionless, corresponding to an effective absorber atom layer spacing divided by the bulk interlayer spacing for the appropriate sets of scatterer planes.

A striking feature of these parameter values is that the coherent fractions for both NIXSW conditions for both V species are low. We note, of course, that for an ultra-thin film of epitaxial VO_2 the coherent positions for both reflections are expected to be close to unity, and that the oxidic component does show such values, so the low coherent fractions clearly indicate that this simple interpretation of the oxidic component cannot be correct. The low coherent fractions clearly indicate that for both the oxidic and metallic surface species there must be at least two distinct local adsorption sites.

In order to identify possible structures consistent with these data we first consider possible V adsorption sites on a perfect TiO_2(110) surface. For the calculations that follow we will assume an ideally terminated bulk structure for the surface; it is well known that the clean TiO_2(110) surface layers suffer significant relaxations, with local displacements of up to ~0.2 Å, although the exact amplitude (and in some cases the sign) of these displacements remains somewhat controversial (see the review by Diebold [41] and the results of two newer experimental studies [42,43]). However, as these relaxations will almost certainly be modified by the presence of the surface V atoms, the bulk termination seems a simpler and equally realistic starting point. As we shall see, relatively subtle substrate relaxations are unlikely to change our main structural conclusions.

Fig. 5 shows a plan view of a schematic model of the surface with some possible V atom adsorption sites identified. In their STM investigation of the earliest stages of V deposition on TiO_2(110), Agnoli et al. [13] focus on two possible sites referred to as the upper and lower 3-fold hollow sites (U3 and L3, respectively hereafter) and specifically identify the U3 sites as those that are preferentially occupied at very low (~0.05 ML) coverage. The U3 site involves 3-fold coordination to surface O atoms, specifically two bridging and one fully coordinated surface plane O atom. The L3 site proposed involved similar 3-fold oxygen coordination, but in this case to one bridging O atom and two surface plane O atoms. A calculation of the bond-lengths associated with this site, however, shows that if we assume V–O bondlengths of 2.0 Å (similar to V–O and Ti–O bondlengths in the rutile phase) the V atom lies only 1.85 Å from the nearest 5-fold coordinated surface Ti atom below. This is much shorter than the expected

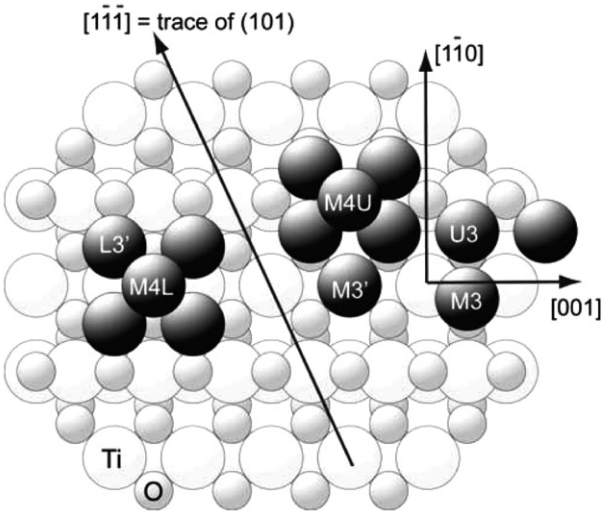

Fig. 5. Schematic plan view of the TiO_2(110) surface showing possible V adsorption sites. The Ti and O atoms are shown as the large and small light-shaded spheres respectively; the V atoms are shown as dark-shaded spheres of similar size to the Ti atoms. Notice that in representations of TiO_2 it is common to represent Ti atoms by smaller spheres than the O atoms, reflecting their relative ionic radii. Here we use touching spheres with radii such that the hard-sphere picture is meaningful to the expected Ti–V and V–V interatomic distances, influenced by the metallic radii.

value of approximately 2.6 Å, so a true L3 site on a bulk-terminated TiO_2(1 1 0) surface is clearly not possible. In Fig. 5 we show instead a site labelled L3′ in which the V atom has been displaced upwards out of the surface to give a V–Ti distance of 2.6 Å and displaced some 0.2 Å parallel to the surface towards the bridging O atom to maintain a V–O bondlength of 2.0 Å. Perhaps the most obvious further V adsorption site involving O bonding is atop the bridging O atoms, as this would correspond to the epitaxial site for pseudomorphic growth of rutile-phase VO_2.

In addition to these adsorption sites in which V atoms are bonded to one or more surface O atoms, Fig. 5 shows four other possible sites in which the bonding is to other metal atoms. The M3 and M3′ sites both have 3-fold coordination to metal atoms, specifically two Ti and one V atom for M3, and two V and one Ti atom for M3′. The M4L and M4U sites correspond to 4-fold coordination to V atoms adsorbed in the L3′ and U3 sites, respectively. Notice that the M4U site is essentially the epitaxial site atop a bridging O atom, although the V–O bondlength is probably slightly longer (∼0.1–0.3 Å) than the nominal value of 2.0 Å we have used for V–O bonding. These four sites, in which the bonding is primarily or exclusively to other metal atoms, seem the most likely candidates to contribute to the metallic component of the V 2p photoemission peaks, while the U3 site (together with epitaxial or Ti substitutional sites) may be expected to contribute to the oxidic component of the V 2p photoemission. Which photoemission peak the V atoms in the L3′ site should contribute to is less clear, but with only a single O near-neighbour, it is reasonable to suggest that the photoemission from such an atom is more likely to contribute to the 'metallic' peak, particularly if the M4L sites are also occupied, thus creating a metal cluster.

Table 2 shows the NIXSW structural parameter values to be expected from these different sites based on a bulk-terminated TiO_2 substrate and assumed V–O and V–Ti nearest neighbour distances of 2.00 Å and 2.60 Å, respectively. Because the NIXSW technique measures the location of adsorbate atoms relative to the extended bulk scatterer plane positions, and not the outermost substrate plane, surface relaxations will modify the predicted coherent position values; however, the offset in these values corresponds to the sum of all outer layer relaxations, which typically change sign between layers leading to some net cancellation, and not to the outermost layer relaxation alone. The impact of these relaxations will be most significant for the (1 1 0) coherent position values and zero or minimal for coherent fraction values. Notice that in all sites the layer spacing perpendicular to the surface is well-defined and single-valued, so the nominal expectation for the (1 1 0) coherent fraction is a value of unity (reduced somewhat, in reality, by static and dynamic disorder). For several of these sites, however, there are distinct but symmetrically equivalent sites (related by the point group symmetry operations of the substrate) which lead to two distinct values for the (1 0 1) coherent position; combining these values leads to an average coherent position value, but in some cases to a substantial reduction in the coherent fraction. This effect is most significant for the U3 and L3′ sites, for which the two symmetrically equivalent sites lie on opposite sides of the bridging oxygen rows. In the case of the L3′ sites, the two contributing values of the (1 0 1) coherent position are 0.10 and 0.55 which differ by 0.45, very close to the value of 0.50 (one half of an interlayer spacing) at which exact cancellation occurs; the resulting coherent fraction is thus only 0.15. For the U3 site this situation is similar but less severe, the (1 0 1) coherent positions differing by 0.36.

Table 2
Expected NIXSW parameter values for different individual adsorption sites (see Fig. 5) of V on TiO_2(1 1 0)

Site	(1 1 0) NIXSW parameters		(1 0 1) NIXSW parameters	
	d_{110}	f_{co}	d_{101}	f_{co}
U3	0.57	1.00	0.28	0.42
L3′	0.66	1.00	0.32	0.15
Epitaxial or substitutional	1.00	1.00	1.00	1.00
M3	0.65	1.00	0.82	0.88
M3′	0.80	1.00	0.40	1.00
M4L	0.14	1.00	0.07	1.00
M4U	0.13	1.00	0.06	1.00

Armed with the information contained in Table 2, we can evaluate the compatibility of various models with the experimental results of Table 1. For the V atoms contributing to the oxide component of the V 2p photoemission peak, the most obvious candidates are V atoms that adopt epitaxial rutile-phase sites including substituting Ti atoms in the near-surface region. These sites would be expected to give coherent position values for both NIXSW conditions close to 1.00 (or equivalently 0.00), and high coherent fraction values ($\gtrsim$ 0.8–0.9). The experimental coherent position values are quite close to this expectation (although d_{101} does differ significantly) but the coherent fractions are low, and particularly low for the (1 1 0) reflection. The clear implication is that if these epitaxial or substitutional sites are occupied (NIXSW does not distinguish these two possibilities), there must also be one (or more) additional sites filled that have the primary effect of reducing the coherent fractions, particularly for the (1 1 0) NIXSW. The U3 site, that we have already identified as probably consistent with the oxidic component of the V 2p photoemission signal, satisfies these requirements. In particular, the associated $d_{1\,1\,0}$ value of 0.57 for this site is almost half a layer spacing different from that of the epitaxial site, so this will produce a strong decrease in the combined coherent fraction but only a modest change in the coherent position. Notice, too, that in the (1 0 1) NIXSW this site alone has a rather low coherent fraction, but a coherent position of 0.28 which, combined with the value of 0.00 for the epitaxial site will produce a small value (i.e. slightly greater than 0.00) for the combined coherent position, in line with the experimental value. Evaluation of a model based on 2/3

of the oxidic V atoms in epitaxial or substitutional sites, and 1/3 in the U3 sites, leads to the following NIXSW parameters: (1 1 0), $d_{110} = 0.94$, $f_{co} = 0.38$; (1 0 1), $d_{101} = 0.03$, $f_{co} = 0.64$. Notice that these coherent fraction values are upper limits, and take no account of static or dynamic disorder. Clearly this model reproduces all the main trends of the experimental data, namely both coherent positions close to unity/zero and substantially reduced coherent fractions, with the value of f_{co} for the (1 1 0) NIXSW being much lower than for the (1 0 1) reflection. The main quantitative discrepancy is in the coherent position for the (1 1 0) reflection, which is somewhat lower than the experimental value. We should stress, however, that this analysis takes no account of possible relaxations at or close to the surface that could account for this level of disagreement.

We now consider the metallic component of the surface vanadium. Here the striking feature of the experimental data is that not only are the coherent fractions low, but the coherent position for the (1 1 0) reflection is 0.64, whereas for the (1 0 1) reflection it is essentially unity (or equivalently, zero). As Table 2 shows, three of the sites considered here have d_{110} values around 0.6, namely U3, L3′ and M3. U3 we have already argued is more likely to contribute to the oxidic peak in the V 2p photoemission, being bonded to three surface O atoms (two of which, the bridging O atoms, are under-coordinated). We therefore do not consider further any contribution of this site to the metallic V. Of the remaining two sites, the properties of the L3′ site are of especial interest because not only is the d_{110} value close to that measured experimentally, but while the d_{101} value is completely different to the experimental value, its associated coherent fraction is very low. Because of this, a mixture with a second site with a high (1 0 1) coherent fraction will show a d_{101} value dominated by the second site. Of course, as in the case of the oxidic species, the low (1 1 0) coherent fraction for the metallic species clearly indicates at least two distinct sites are occupied, and here too a second site with a d_{110} value that differs from the L3′ site by approximately 0.50 will lead to a strong suppression of the coherent fraction. Two possible sites fit this requirement, M4L and M4U. The NIXSW parameters expected for these two sites are essentially identical, so either one or a mixture of the two will have the same effect. For simplicity we consider first only the M4L site, but will return to this ambiguity below.

For a solution based on co-occupation of the L3′ and M4L sites, we note that as the M4L sites occupy 4-fold coordinated hollow sites on top of the L3′ sites, the occupation of the M4L sites must be lower. For extended rows of both sites, the occupation of the M4L sites will be one half that of the L3′ sites. Consider, therefore, a model based on 2/3 L3′ sites and 1/3 M4L sites. For this combination the predicted NIXSW parameter values are: (1 1 0), $d_{110} = 0.68$, $f_{co} = 0.34$; (1 0 1), $d_{101} = 0.11$, $f_{co} = 0.34$. In this case the only parameter lying outside the experimental error estimates is d_{101}, and here too modest changes in the assumed relaxations and interatomic spacings could account to this discrepancy. An increase of a few percent in the occupation of the M4 sites is slightly favoured in that it lowers d_{110}, lowers the coherent fraction for (1 1 0) and raises the coherent fraction for (1 0 1), but has rather little effect on d_{101}. Of course, raising the proportion of M4 sites above one half of that of the L3′ sites clearly requires some occupation of the M4U site as well as the M4L site. Notice that the majority occupation of the L3′ site in this model carries with it the implicit assumption that the L3′ site, with one near-neighbour O atom, has an associated V 2p chemical shift characteristic of the 'metallic' component of the photoemission experiment. Bearing this in mind, it is certainly reasonable to assume that both the M4L and M4U sites, with entirely or almost entirely V nearest-neighbours, also contribute to the metallic state. While this structural model of the metallic component of the sub-monolayer coverage of V on TiO_2(1 1 0) appears adequate to explain the experimental data, we cannot exclude some minor contribution from other sites. In particular, the M3 site would give a similar effect on the (1 1 0) structural parameters as the L3′ site, but while a small admixture of this site would lead to a lowering of d_{110}, consistent with experiment, this site cannot replace the L3′ site in the mixture, as this leads to a high coherent fraction for the (1 0 1) NIXSW.

3.3. Multilayer growth of VO_x on TiO_2(1 1 0)

The main results of the investigation of the thin VO_x films, grown by the two methods of post-oxidation and reactive evaporation, in the form of NIXSW (1 1 0) structural parameters, are summarised in Table 3, each row corresponding to similar estimated film thicknesses. As noted earlier, these film thickness values are indicative only, in that they take no account of possible differences in film morphology. Nevertheless, there are clear trends as a function of film thickness and in terms of the relative properties of films prepared by the two different methods. For ideal pseudomorphic growth of rutile phase VO_2 we would anticipate that the slightly larger lattice parameters of

Table 3
Summary of (1 1 0) NIXSW parameters for films of VO_x grown on TiO_2(1 1 0) by the two alternative growth modes

Post-oxidation growth (PO)			Reactive evaporation growth (RE)		
Film thickness (MLE)	d_{110}	f_{co}	Film thickness (MLE)	d_{110}	f_{co}
0.5	0.99	0.75	0.5	0.97	0.66
1.0	0.97	0.89	1.0	0.98	0.58
			1.6	0.96	0.64
2.7	0.93	0.33	2.4	0.90	0.33
			3.5	0.82	0.19
6.8	0.89	0.20	5.6	(0.35)	0.02
10.0	0.86	0.15			

The two data sets are presented in such a way that data for similar film thicknesses appear in each row. The coherent position value for the thickest RE film is bracketed because, with an associated coherent fraction value of 0.02, the coherent position is essentially meaningless. Typical precision estimates are ~±0.02–0.04 in d_{110} and ~±0.05–0.10 in f_{co}.

TiO_2, particularly in the [0 0 1] azimuthal direction, and the associated elastic strain, would lead to an interlayer spacing of the VO_2 approximately 2% smaller than of the underlying TiO_2 in which the standing wavefield is established. On this basis, neglecting all surface relaxations and specific interface effects, one might expect d_{110} from the V atoms to have a value of approximately 0.98 for the first monolayer with a high associated coherent fraction. Successive layers would then become further and further displaced from the extended Ti scatterer plane positions, so after 10 layers deposited in this idealised model the outermost V layer would have a location corresponding to a d_{110} value of 0.80. Of course, for this thicker film the V 2p photoemission signal used to monitor the absorption arises from many layers, so the contributions of each layer would contribute coherent position values between 0.98 and 0.80, leading to some average value weighted to the value of the outermost layers. This range of values would also lead to some reduction in the associated coherent position, but even if all 10 layers contributed equally the expected resulting reduction in the coherent fraction is only 6%.

Inspection of the experimental results of Table 1 shows the qualitative trends correspond to this simple picture, but the quantitative effect is much more pronounced, particularly with regard to the coherent fraction which falls far more steeply with increasing film thickness than anticipated. A clear conclusion is that the thicker films, in particular, have a quality far short of ideal pseudomorphic growth of rutile-phase VO_2. It is also notable that for a given film thickness the quality of the film, as judged by the NIXSW (1 1 0) coherent fraction, is inferior when grown by the RE method to that of films grown by the PO method, a conclusion in qualitative agreement with the results of the early work by the Granozzi group.

Before considering the results for the thicker films in more detail we should first note that for the films of thickness ~1 MLE or less, the NIXSW data are consistent with generally good epitaxial growth. For the PO growth mode, at least, these ultra-thin films yield coherent positions close to unity/zero and reasonably high coherent fractions for both the (1 1 0) and (1 0 1) (see Table 4) reflection conditions. These ultra-thin films are grown by the post-oxidation and annealing of initial V layers similar to the nominal 0.3 MLE as-deposited film described in the previous section. Post-oxidation not only leads to conversion of the metallic V $2p_{3/2}$ photoemission component to an oxidic photoelectron binding energy, but the NIXSW data show that the remaining oxidic component is now dominated by epitaxial (or substitutional) vanadium atom sites. However, the fact that the (1 1 0) coherent fraction is around 0.75 suggests that there may still be a minor contribution from V atoms chemisorbed in the U3 sites.

Table 4
Summary of fuller NIXSW study of VO_x films grown on TiO_2(1 1 0) by the RE and PO methods on which both (1 1 0) and (1 0 1) measurements were made

Thickness (MLE)	Post-oxidation growth (PO)				Reactive evaporation growth (RE)			
	d_{110}	f_{co}	d_{101}	f_{co}	d_{110}	f_{co}	d_{101}	f_{co}
0.5	0.99	0.75	0.99	0.87	0.97	0.66	0.01	0.70
1.5	0.97	0.70	0.01	0.70	0.94	0.46	0.02	0.52
5.6					0.35	0.02	1.15	0.34

Precision estimates are as in Table 3.

In considering the results for the thicker VO_x films, the small number of measurements of the (1 0 1) NIXSW from selected films, shown in Table 4, is potentially important. Particularly striking is that the 5.6 MLE film grown by the RE method, with a (1 1 0) coherent fraction essentially equal to zero (the optimum fit produced a value of 0.02), has a (1 0 1) coherent fraction of 0.34: very significantly greater than zero. Superficially, the (1 1 0) NIXSW indicates that this film is completely disordered, but the (1 0 1) NIXSW shows that there is a significant degree of spatial coherence (and thus crystallinity) relative to the underlying TiO_2 lattice. We have therefore explored possible alternative crystalline forms of VO_2 which might grow on the surface. The most obvious possibility is that, in addition to pseudomorphic VO_2, crystallites of V_2O_3 are also formed. As remarked earlier, the associated V 2p photoelectron binding energy could be regarded as indicative of such a mixture, and indeed the large width of these photoemission peaks for our films strongly suggest such inhomogeneity. In this regard, it is interesting to note that the inter-planar spacing of the $\{1\,1\,\bar{2}\,0\}$ planes of V_2O_3 is 2.47 Å, almost identical to the value (2.49 Å) for the (1 0 1) planes of TiO_2. It transpires that if one rotates a V_2O_3 crystal away from the (0 0 0 1) basal plane by 25°, about a $\langle 1\,1\,\bar{2}\,0\rangle$ direction, and aligns this along the $[1\,\bar{1}\,1]$ direction within the TiO_2(1 1 0) surface, one finds a good (albeit long-range) coincidence between the two structures in the perpendicular ($[1\,\bar{1}\,5]$) azimuth. In this arrangement the V_2O_3 $\{1\,1\,\bar{2}\,0\}$ are just 2° from the (1 0 1) standing wave nodal planes; for small crystallites, only a few atomic spacings across, the V atoms will thus be coherent with the standing wavefield. Of course, the associated d_{101} value would depend on the exact registry at the interface. Moreover, there would be two rotationally equivalent orientations of these V_2O_3 crystallites, only one of which would have the necessary coherence with the (1 0 1) standing wavefield in the experiment, so half the crystallites would only contribute an incoherent component to the (1 0 1) NIXSW. Nevertheless, such a model does provide one possible means of achieving a (1 0 1) coherent fraction significantly larger than zero. Notice in this interfacial geometry the spacing of the vanadium double-layers within the V_2O_3 crystals relative to the TiO_2(1 1 0) NIXSW nodal planes is only 1.04 Å, compared with the nodal plane spacing of 3.25 Å, so a summation over V atoms in a few such planes will lead to an essentially zero coherent fraction for the (1 1 0) NIXSW. With the limited information available, refinement or even convincing evidence of the correct-

ness of this model is not possible, but it does raise the possibility of partial formation of V_2O_3 crystallites in the thicker films.

4. General discussion and conclusions

While the NIXSW method is limited in that it provides structural information on the location of atoms relative to an extended substrate lattice, and not the local environment of these atoms, it is capable of being applied to both sub-monolayer adsorbate species and thin films, and unlike many methods it provides a quantitative measure of disorder. In the present case the application of the method to identify the adsorption site of an initial sub-monolayer coverage of V atoms can be interpreted in terms of rather specific structural models. As seen in previously reported studies, this type of surface preparation leads to the identification of V atoms in two distinct chemical states as indicated by the V 2p photoemission spectrum, one 'oxidic' and the other 'metallic' in character. Neither state has an associated photoelectron binding energy exactly consistent with either bulk VO_2 or bulk metallic vanadium, but the measured values are sufficiently close to these reference values to support these indicative labels. In the case of the oxidic species, earlier XPD experiments have identified the associated V atoms as occupying Ti substitutional sites in the surface layer [7]. Our NIXSW results show that while a significant fraction (up to 2/3) of the 'oxidic' V atoms do occupy sites which could be either substitutional or epitaxial, these sites alone cannot account for the data. Co-occupation of the U3 site, a chemisorption site with three oxygen nearest-neighbour atoms (two bridging, one in-plane), can however, account for the NIXSW results. It is notable that occupation of this 'upper 3-fold hollow' site had been previously identified at very low (~0.05 ML) coverage in STM studies [13], but the STM data do not, of course, identify the chemical state (or even the elemental character) of these atoms. Our results clearly indicate that these V atoms contribute to the oxidic state, a conclusion consistent with the 3-fold coordination to O atoms (two of which are under-coordinated in the $TiO_2(1\,1\,0)$ surface). Indeed, it is possible that it is the contribution from these U3 V atoms which leads to the associated V 2p photoelectron binding energy being slightly different from that of the thicker oxide films.

In the case of the metallic surface V atoms, at least two local adsorption sites are necessary to account for the NIXSW results. One of these is some kind of second-layer V deposit (for which two alternative sites appear equally possible and may both contribute), but the other is a second chemisorption site on the bare $TiO_2(1\,1\,0)$ surface; this L3′ site has a single O atom and a single Ti atom as its nearest neighbours. The fact that a significant fraction of second-layer V atoms are involved, thus implying the formation of metallic clusters, is also consistent with STM observations of the TiO_2 surface following V deposition to higher sub-monolayer coverages [13].

The second set of measurements reported here relate to ultrathin films of VO_x grown in two different ways with the objective of trying to produce pseudomorphic rutile-phase VO_2 films with thicknesses up to about 6 MLE. The NIXSW data show that most of these films fall far short of this ideal in their crystalline quality or character. For the very thinnest films (less than or about 1 MLE), particularly grown by the PO method, NIXSW indicates that the great majority of the V atoms do adopt sites consistent with this ideal. Strictly, NIXSW cannot distinguish whether the V sites are epitaxial or substitutional, and there may be some intermixing of the V and Ti atoms in the outermost surface layers, although the slight tendency for the $(1\,1\,0)$ coherent position to take a value fractionally less than unity could be taken to favour an epitaxial overlayer. These layers may also retain a small fraction of chemisorbed V atoms in the U3 sites on the TiO_2 surface.

For the thicker films, the coherent fractions rapidly fall with increasing thickness, such that for a film of 5.6 MLE grown by RE the $(1\,1\,0)$ coherent fraction is essentially zero, although the situation is slightly better for films grown using the PO method. One could, perhaps, attribute this to a growing content of amorphous or randomly oriented crystallites. Surprisingly though, even for the 5.6 MLE RE-grown film mentioned above, the $(1\,0\,1)$ coherent fraction is significant (0.34), implying that there is a clear crystalline component that is no longer coherent with the extended $(1\,1\,0)$ lattice planes. One possible explanation for this is a growing component of V_2O_3 crystallites for which a particular interfacial structure (outlined above) offers some possibility of accounting for the available data. That the films are rather inhomogeneous is supported by the broad V 2p photoemission spectra from the thicker films (see Fig. 2) which could certainly accommodate two distinct chemically shifted components.

The implication of this interpretation would be that the RE growth mode favours V_2O_3 formation more than the PO mode, and that in both modes the growth of V_2O_3 is favoured at larger film thicknesses. Under the particular conditions used for these two growths in these experiments there are significant differences in oxygen supply, and we surmise that this may well be the cause of the difference. In the PO growth procedure each aliquot of V atoms was exposed to 1×10^{-6} mbar oxygen for 2 min at a substrate temperature of ~200 °C, but in the RE mode the V atoms were deposited at a steady rate over a period of only 1 min in a lower (5×10^{-8} mbar) partial pressure of oxygen. These conditions for the RE growth were chosen to be similar to those found to produce superior films in the earlier STM studies [14]. The average oxygen flux seen by the surface V atoms is thus almost two orders of magnitude higher in the PO growth. We note, however, that in the RE growth experiments the rate of arrival of O_2 molecules at the surface was approximately three times that of the V atoms, so one might have expected that this would be more than adequate to ensure 'complete' oxidation if the sticking factor is close to unity. The formation of the VO_2 is also

favoured by epitaxy with the substrate, and for this epitaxial growth surface mobility is important; the fact that the as-deposited V surface was exposed to oxygen for twice as long at the PO annealing temperature, as the deposition time in the RE growth, may be a further factor favouring improved VO_2 epitaxy. On the other hand, the fact that in RE growth the oxygen is available while the surface V atoms are 'hot', as they are accommodated onto the surface, might be expected to favour better epitaxy in RE growth.

In general, an important conclusion of these studies is that neither PO nor RE VO_x growth on $TiO_2(1\,1\,0)$, at least under the conditions used here, leads to good quality VO_2 films except, perhaps, for the first monolayer. For these ultrathin films, however, significant intermixing of Ti and V at the interface may occur (as indicated by the earlier XPD studies), and NIXSW does not distinguish between epitaxial and substitutional V. We should perhaps stress that our results are not inconsistent with earlier studies by other methods. Most notably, XPD studies of PO growth under conditions closely similar to those that we have used indicates the formation of epitaxial VO_2. Our results are perfectly consistent with some fraction of the film having this property, but other parts involving some other phase, probably V_2O_3 crystallites with several different orientations, the basal plane being strongly tilted relative to the $TiO_2(1\,0\,1)$ surface. Under these conditions it is likely that the XPD would show the forward scattering features expected of the single-orientation VO_2, whereas the non-epitaxial components would contribute only a relatively isotropic background. Our results are also consistent with the apparent absence of good long-range order manifested in the absence of good LEED patterns from these films.

Acknowledgement

The authors acknowledge the financial support of the Physical Sciences and Engineering Research Council (UK) and of the Deutsche Forschungsgemeinschaft through the Sonderforschungsbereich 546. They also acknowledge the award of beamtime on the SRS by CCLRC, and the benefit of useful discussions with Victor Henrich.

References

[1] V.E. Henrich, P.A. Cox, The Surface Science of Metal Oxides, Cambridge University Press, Cambridge, 1994.
[2] K. Hermann, M. Witko, in: D.P. Woodruff (Ed.), The Chemical Physics of Solid Surfaces: Oxide Surfaces, vol. 9, Elsevier Science, Amsterdam, 2001.
[3] B.M. Weckhuysen, D.E. Keller, Catal. Today 78 (2003) 25.
[4] S. Surnev, M.G. Ramsey, F.P. Netzer, Prog. Surf. Sci. 73 (2003) 117.
[5] Z. Zhang, V.E. Henrich, Surf. Sci. 277 (1992) 263.
[6] M. Sambi, E. Pin, G. Sangiovanni, L. Zaratin, G. Granozzi, F. Parmigiani, Surf. Sci. 349 (1996) L169.
[7] M. Sambi, G. Sangiovanni, G. Granozzi, F. Parmigiani, Phys. Rev. B 54 (1996) 13464.
[8] M. Sambi, G. Sangiovanni, G. Granozzi, F. Parmigiani, Phys. Rev. B 55 (1997) 7850.
[9] M. Della Negra, M. Sambi, G. Granozzi, Surf. Sci. 436 (1999) 227.
[10] M. Sambi, M. Della Negra, G. Granozzi, Z.S. Li, J.H. Jørgensen, P.J. Møller, Appl. Surf. Sci. 142 (1999) 146.
[11] M. Sambi, M. Della Negra, G. Granozzi, Surf. Sci. 470 (2000) L116.
[12] M. Sambi, M. Della Negra, G. Granozzi, Thin Solid Films 400 (2001) 26.
[13] S. Agnoli, C. Castellarin-Cudia, M. Sambi, S. Surnev, M.G. Ramsey, G. Granozzi, F.P. Netzer, Surf. Sci. 546 (2003) 117.
[14] S. Agnoli, M. Sambi, G. Granozzi, C. Castellarin-Cudia, S. Surnev, M.G. Ramsey, F.P. Netzer, Surf. Sci. 562 (2004) 150.
[15] Q. Guo, W.S. Oh, D.W. Goodman, Surf. Sci. 437 (1999) 38.
[16] N.J. Price, J.B. Reitz, R.J. Madix, E.I. Solomon, J. Electron Spectr. Rel. Phenom. 98–99 (1999) 257.
[17] J. Biener, M. Bäumer, J. Wang, R.J. Madix, Surf. Sci. 450 (2000) 12.
[18] Z. Chang, S. Piligkos, P.J. Møller, Phys. Rev. B 64 (2001) 165410.
[19] G.S. Wong, M.R. Concepcion, J.M. Vohs, Surf. Sci. 526 (2003) 211.
[20] G.A. Sawatzky, D. Post, Phys. Rev. B 20 (1979) 1546.
[21] G. Silversmit, D. Depla, H. Poelman, G.B. Marin, R. De Gryse, J. Electron Spectr. Rel. Phenom. 135 (2004) 167.
[22] Q. Wang, R.J. Madix, Surf. Sci. 474 (2001) L213.
[23] D.P. Woodruff, A.M. Bradshaw, Rep. Prog. Phys. 57 (1994) 1029.
[24] D.P. Woodruff, Prog. Surf. Sci. 57 (1998) 1.
[25] D.P. Woodruff, Rep. Prog. Phys. 68 (2005) 743.
[26] V.R. Dhanak, A.W. Robinson, G. van der Laan, G. Thornton, Rev. Sci. Instr. 63 (1992) 1342.
[27] A.W. Robinson, S. D'Addato, V.R. Dhanak, P. Finetti, G. Thornton, Rev. Sci. Instr. 66 (1995) 1762.
[28] L.-Q. Wang, D.R. Baer, M.H. Engelhard, A.N. Shultz, Surf. Sci. 344 (1995) 237.
[29] C.J. Powell, A. Jablonski, NIST Electron Effective-Attenuation-Length Database, NIST, Gaithersburg, MD, 2003.
[30] J. Zegenhagen, Surf. Sci. Rep. 18 (1993) 199.
[31] D.P. Woodruff, D.L. Seymour, C.F. McConville, C.E. Riley, M.D. Crapper, N.P. Prince, R.G. Jones, Phys. Rev. Lett. 58 (1987) 1460.
[32] M. Sugiyama, S. Maeyama, S. Heun, M. Oshima, Phys. Rev. B 50 (1995) 14778.
[33] G.J. Jackson, D.P. Woodruff, R.G. Jones, N.K. Singh, A.S.Y. Chan, B.C.C. Cowie, V. Formoso, Phys. Rev. Lett. 84 (2000) 119.
[34] G.J. Jackson, J. Lüdecke, D.P. Woodruff, A.S.Y. Chan, N.K. Singh, J. McCombie, R.G. Jones, B.C.C. Cowie, V. Formoso, Surf. Sci. 441 (1999) 515.
[35] C.J. Fisher, R. Ithin, R.G. Jones, G.J. Jackson, D.P. Woodruff, B.C.C. Cowie, J. Phys.: Condens. Matter 10 (1998) L623.
[36] I.A. Vartanyants, J. Zegenhagen, Solid State Commun. 113 (1999) 299.
[37] J. Lee, C. Fisher, D.P. Woodruff, M.G. Roper, R.G. Jones, B.C.C. Cowie, Surf. Sci. 494 (2001) 166.
[38] D.P. Woodruff, B.C.C. Cowie, A.R.H.F. Ettema, J. Phys.: Condens. Matter 6 (1994) 10633.
[39] V.I. Nefedov, V.G. Yarzhemsky, I.S. Nefedova, M.B. Trzhaskovskaya, I.M. Band, J. Electron Spectros. Rel. Phenom. 107 (2000) 123.
[40] V.E. Henrich, in: R.St.C. Smart, J. Notwotny (Eds.), Ceramic Interfaces: Properties and Applications, Inst. Metals, London, 1998, p. 31.
[41] U. Diebold, Surf. Sci. Rep. 48 (2003) 53.
[42] R. Lindsay, A. Wander, A. Ernst, B. Montanari, G. Thornton, N.M. Harrison, Phys. Rev. Lett. 94 (2005) 246102.
[43] G.S. Parkinson, M.A. Muñoz-Márquez, P.D. Quinn, M.J. Gladys, R.E. Tanner, D.P. Woodruff, P. Bailey, T.C.Q. Noakes, Phys. Rev. B 73 (2006) 245409.